A full circuit-based quantum algorithm for excited-states in quantum chemistry

Jingwei Wen[1,2], Zhengan Wang[3], Chitong Chen[4,5], Junxiang Xiao[1], Hang Li[3], Ling Qian[2], Zhiguo Huang[2], Heng Fan[3,4], Shijie Wei[3], and Guilu Long[1,3,6,7]

[1]State Key Laboratory of Low-Dimensional Quantum Physics and Department of Physics, Tsinghua University, Beijing 100084, China
[2]China Mobile (Suzhou) Software Technology Company Limited, Suzhou 215163, China
[3]Beijing Academy of Quantum Information Sciences, Beijing 100193, China
[4]Institude of Physics, Chinese Academy of Sciences, Beijing 100190, China
[5]School of Physical Sciences, University of Chinese Academy of Sciences, Beijing 100190, China
[6]Frontier Science Center for Quantum Information, Beijing 100084, China
[7]Beijing National Research Center for Information Science and Technology, Beijing 100084, China

Utilizing quantum computer to investigate quantum chemistry is an important research field nowadays. In addition to the ground-state problems that have been widely studied, the determination of excited-states plays a crucial role in the prediction and modeling of chemical reactions and other physical processes. Here, we propose a non-variational full circuit-based quantum algorithm for obtaining the excited-state spectrum of a quantum chemistry Hamiltonian. Compared with previous classical-quantum hybrid variational algorithms, our method eliminates the classical optimization process, reduces the resource cost caused by the interaction between different systems, and achieves faster convergence rate and stronger robustness against noise without barren plateau. The parameter updating for determining the next energy-level is naturally dependent on the energy measurement outputs of the previous energy-level and can be realized by only modifying the state preparation process of ancillary system, introducing little additional resource overhead. Numerical simulations of the algorithm with hydrogen, LiH, H2O and NH3 molecules are presented. Furthermore, we offer an experimental demonstration of the algorithm on a superconducting quantum computing platform, and the results show a good agreement with theoretical expectations. The algorithm can be widely applied to various Hamiltonian spectrum determination problems on the fault-tolerant quantum computers.

Jingwei Wen: wjw17@tsinghua.org.cn
Shijie Wei: weisj@baqis.ac.cn
Guilu Long: gllong@tsinghua.edu.cn

1 Introduction

As one of the emerging research fields, quantum computation is devoted to solving some certain computational problems that are intractable to deal with in classical computers using the principles of quantum mechanics [1, 2]. Since the concept was proposed, quantum computing has become one of the most fruitful fields in contemporary physics and various important problems of practical significance such as prime factorization [3], database search [4, 5], and solution of linear equations [6, 7] have been solved by algorithms in quantum version. In recent years, the development of quantum algorithms applied to quantum chemistry have become an active research field, with huge potential market application value [8, 9, 10]. Some quantum algorithms used to determine the ground-state of chemical molecule Hamiltonian, such as the classical-quantum hybrid variational quantum eigensolver (VQE) algorithm [11, 12, 13, 14] and its improvements [15, 16, 17, 18], the full quantum eigensolver (FQE) algorithm [19], have obtained rapid

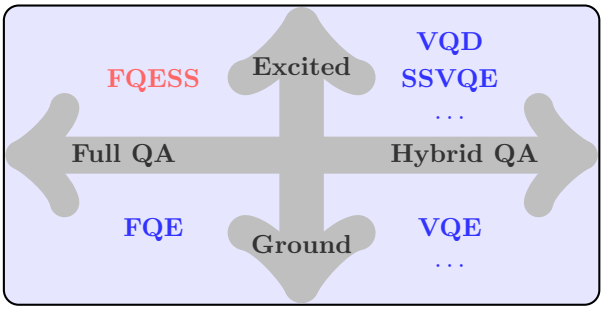

Figure 1: Classification of quantum algorithms for quantum chemistry. The algorithms are divided into hybrid quantum algorithm for noisy intermediate scale quantum (NISQ) devices and full quantum algorithm for fault-tolerant quantum computers, where the former one requires the cooperation of classical and quantum computers while the latter one is based on the full circuit-based quantum operation. The purpose of quantum chemistry is divided into determining ground- or excited-states.

theoretical development and some state-of-the-art experimental demonstration. To be specific, the VQE algorithm is divided into two parts, i.e. preparing and measuring of quantum states on the quantum computer and parameter optimization on the classical computer. By iterating the whole process until convergence, the ground-state and ground-state energy of the target Hamiltonian can be obtained. But the FQE algorithm removes the classical optimizer and performs all the calculations on the quantum computer by using quantum gradient descent [20].

However, in addition to the ground-states, the determination of the excited-states is also indispensable for the study of chemical reaction processes. Up to now, a series of modified versions of the hybrid variational algorithms have been proposed for finding energy spectrum, such as variational quantum deflation (VQD) [21, 22] and subspace-search variational quantum eigensolver (SSVQE) [23, 24] algorithms and some extension versions [25, 26, 27, 28, 29, 30, 31]. The basic idea of the former method is introducing state-specific penalization terms to the Hamiltonian and determining each eigenstate by a separate minimization. While the latter algorithm performs a single minimization for a set of initially selected orthogonal states with one ansatz, and realizes the mapping from these states to the lower excited-states of target Hamiltonian.

Although so much progress has been made in the investigation of excited-states, it is still a research direction of concern to determine the energy spectrum of the molecular Hamiltonian based on a complete quantum circuit model for future fault-tolerant quantum computation, just as shown in the Figure 1. In this work, we fill the last step of solving quantum chemistry problems in different algorithm frames and propose a full quantum excited-state solver (FQESS) algorithm for determining the whole spectrum of chemistry Hamiltonian efficiently and steadily. Compared with classical-quantum hybrid variational algorithms, our method removes the optimization in classical computers, and its non-variational nature can ensure that the algorithm converges to the target states along the direction of the fastest gradient descent, avoiding barren plateau phenomenon. Moreover, the parameter updating for different energy-levels can be simply realized by modifying the state preparation process of ancillary system based on the energy measurement of the last energy-level, which is experimentally friendly.

This paper is organized as follows: in Sec 2, we introduce the details of the FQESS algorithm, and analyze the complexity of the algorithm. In Sec 3, we present a numerical simulation with hydrogen, LiH, H2O and NH3 molecules under noiseless and noise condition separately. In Sec 4, we offer an experimental demonstration of FQESS algorithm on the real superconducting quantum computing platform. Finally, sec 5 gives a conclusion.

2 Results

2.1 Full Quantum Excited-State Solver

Here we introduce a full quantum algorithm for solving the excited-states of the quantum chemistry Hamiltonian. Quantum simulation of fermionic systems can be reformulated in terms of qubit operations by Jordan-Wigner [32] or Bravyi-Kitaev transformation [33], and then the target n-qubit chemistry Hamiltonian can be generally expressed as

$$H_1 = \sum_{i=1}^{L_1} \alpha_i^{(1)} P_i \tag{1}$$

which is expressed as the linear combination of $L_1 \leq 4^n$ Pauli words P_i (tensor product of Pauli matrices) with real coefficients $\alpha_i^{(1)}$, and we want

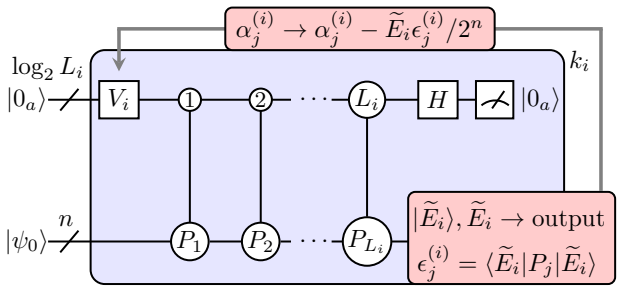

Figure 2: Quantum circuit for the realization of FQESS algorithm. The whole system includes $n+\log_2 L_i$ qubits and is divided into working system and ancillary system. The basic process for determining the i-th eigenstate, which is repeated by k_i times, includes four parts, that is encoding with operator V_i, entangling with L_i controlled gates, decoding with Hardmard gates and measurement on the ancillary qubits. The output state of working system is $\left|\widetilde{E}_i\right\rangle$ and its measurement results on the different Pauli words $\epsilon_j^{(i)}$ is used for calculating the eigenvalues $\widetilde{E}_i$ and updating the state preparation operator.

to find the spectrum. Let the set of eigenstates be $\{|E_j\rangle\}_{j=1}^{2^n}$ with corresponding eigenenergies $\{E_j\}_{j=1}^{2^n}$, satisfying $|E_i| \geq |E_j|$ when $i \leq j$.

We first need to construct a quantum circuit to realize the Hamiltonian in equation (1), as shown in the Figure 2. Note that we have n-qubit as the working system, while we need another $\log_2 L_1 \leq 2n$ qubits as the ancillary system. In principle, we at most need $3n$ qubits to ensure the expansion generality of the subsequent quantum states. The details for the realization of such a process with quantum circuits will be presented in section 2.2. Once we realize the Hamiltonian H_1 with the quantum circuit, we apply the circuit-based operators with enough times (k_1 times) to an arbitrary initial quantum state $|\psi_0\rangle$, then we have the normalized quantum state as $\left|\widetilde{E}_1\right\rangle = H_1^{k_1}|\psi_0\rangle / (\langle\psi_0| H_1^{2k_1} |\psi_0\rangle)^{1/2}$, an approximation to the eigenvector $|E_1\rangle$ with the biggest absolute value of eigenvalue $|E_1|$. The corresponding approximate eigenvalue $\widetilde{E}_1$ can be determined by $\widetilde{E}_1 = \left\langle \widetilde{E}_1 \right| H_1 \left| \widetilde{E}_1 \right\rangle = \sum_{i=1}^{L_1} \alpha_i^{(1)} \epsilon_i^{(1)}$, and the energy component $\epsilon_i^{(1)} = \left\langle \widetilde{E}_1 \right| P_i \left| \widetilde{E}_1 \right\rangle$ can be obtained by measuring the average values of the output quantum state under different Pauli words.

Furthermore, based on the completeness of Pauli basis, output density matrix $\rho_1 = \left|\widetilde{E}_1\right\rangle\left\langle\widetilde{E}_1\right|$ can be expanded as $\rho_1 = \sum_{j=1}^{l_1} \beta_j^{(1)} P_j$, where the coefficients satisfy $\beta_j^{(1)} = \mathrm{tr}(P_j\rho_1)/2^n = \epsilon_j^{(1)}/2^n$. This can be understood as the energy contribution of ρ_1 to each Pauli term in the Hamiltonian. Then we can re-constructed the original Hamiltonian as

$$H_2 = \sum_{i=1}^{L_2} (\alpha_i^{(1)} - \widetilde{E}_1 \beta_i^{(1)}) P_i = \sum_{i=1}^{L_2} \alpha_i^{(2)} P_i \qquad (2)$$

which can be realized with the same circuit as above, just changing the initial state preparation of ancillary system. The corresponding physical meaning is that we have eliminated the energy contribution of $|E_1\rangle$ to each Pauli term in the Hamiltonian, so the biggest absolute value of eigenvalues for the new Hamiltonian is $|E_2|$ now. Similarly, by applying the new circuit-based operator with k_2 times to the arbitrary initial quantum state, we can have

$$\left|\widetilde{E}_2\right\rangle = \frac{H_2^{k_2}|\psi_0\rangle}{\sqrt{\langle\psi_0| H_2^{2k_2} |\psi_0\rangle}}, \quad \widetilde{E}_2 = \sum_{i=1}^{L_2} \alpha_i^{(2)} \epsilon_i^{(2)} \qquad (3)$$

which is the eigenvector $|E_2\rangle$ with the second biggest absolute value of eigenvalue in H_1 and corresponding eigenvalue E_2.

Repeat this process with 2^n times, we can determine the whole spectrum of the initial Hamiltonian. Note that the order of solution is based on the magnitude of the absolute values of the eigenvalues, rather than the magnitude of the eigenvalues themselves, which may cause some confusion. This can be solved by introducing a bias term $-\lambda_0 I^{\otimes n}$ ($\lambda_0 > \max\{0, E_1, \cdots E_{2^n}\}$) into the Hamiltonian, making all the eigenvalues negative. Then the first solved eigenstate is the ground-state, followed by the first excited-state, and so on. And the bias parameter λ_0 should not be too big, because it affects the ratio of reconstructed eigenvalues $(E_i - \lambda_0)/(E_1 - \lambda_0)$, which is related to the convergence rate of the algorithm. In general, the bigger the bias parameter is, the more operation times we need. The repetition satisfies $k_i = \mathcal{O}(\log(N/\epsilon))$, which is logarithmically dependent on the system size N and the inverse of energy precision ϵ [19]. The FQESS algorithm proposed here can be integrated into the scope of power iteration scheme or quantum gradient descent scheme for eigenvalue evaluation, as discussed in the appendix A. The detailed process of the FQESS algorithm is summarized in the table of Algorithm 1.

Algorithm 1: FQESS algorithm

Input: Hamiltonian $H_1 = \sum_{j=1}^{L_1 \leq 4^n} \alpha_j^{(1)} P_j$, State $|\psi_0\rangle$, Bias parameter λ_0, Iteration times k_i

Output: Eigenstates $\left|\widetilde{E}_i\right\rangle$, Eigenvalues $\widetilde{E}_i$

Preprocess: Construct $U_1 = H_1 - \lambda_0 I^{\otimes n}$

for $i = 1 : 2^n$ **do**

- Apply circuit k_i times to $|\psi_0\rangle$, having $\left|\widetilde{E}_i\right\rangle = U_i^{k_i} |\psi_0\rangle$;
- Measure $\epsilon_j^{(i)} = \left\langle \widetilde{E}_i \right| P_j \left| \widetilde{E}_i \right\rangle$ and get $\widetilde{E}_i = \sum_{j=1}^{L_i} \alpha_j^{(i)} \epsilon_j^{(i)}$;
- **return** $\left|\widetilde{E}_i\right\rangle$ and $\widetilde{E}_i$;
- Reconstruct $\alpha_j^{(i+1)} = \alpha_j^{(i)} - \widetilde{E}_i \epsilon_j^{(i)} / 2^n$;
- Construct circuit $U_{i+1} = \sum_{j=1}^{L_{i+1}} \alpha_j^{(i+1)} P_j - \lambda_0 I^{\otimes n}$

end

2.2 Realization of Circuit-Based Operator

Now we turn to discuss concretely about how to realize the operator $U_i = H_i - \lambda_0 I^{\otimes n}$ in the circuit-based quantum computation frame. Without loss of generality, we can set $P_1 = I^{\otimes n}$, then we have

$$U_i = (\alpha_1^{(i)} - \lambda_0) I^{\otimes n} + \sum_{j=2}^{L_i} \alpha_j^{(i)} P_j \tag{4}$$

where $L_i \leq 4^n$. This is the target operator we aimed to repeat by k_i times when determining the i-th eigenstate. In principle, it can be understood as a linear combination of unitary Pauli words and can be simulated by introducing ancillary qubits to form a bigger Hilbert space [34, 35, 36, 37, 38, 39], as shown in the Figure 2. The basic process is divided into four parts, including encoding, entangling, decoding and measurement. The first encoding process is a quantum state preparation process for ancillary system, realized by the $\log_2 L_i$-qubit operator V_i, whose first column is $[\alpha_1^{(i)} - \lambda_0, \alpha_2^{(i)}, \cdots, \alpha_{L_i}^{(i)}]$. It does not matter what the other matrix elements are as long as the operator is unitary, and we can determine the operator by schmidt orthogonalization or by decomposing it into single- and two-qubit operators. Selectively, the quantum state of ancillary system after encoding is

$$V_i |0_a\rangle = \left[(\alpha_1^{(i)} - \lambda_0) |1\rangle + \sum_{j=2}^{L_i} \alpha_j^{(i)} |j\rangle \right] / \mathcal{C} \tag{5}$$

where $\mathcal{C} = \left[(\alpha_1^{(i)} - \lambda_0)^2 + \sum_{j=2}^{L_i} (\alpha_j^{(i)})^2 \right]^{1/2}$ is a normalization constant. Note that the notations $|0_a\rangle$ and $|1\rangle$ refer to the same quantum states $\left|0^{\otimes \log_2 L_i}\right\rangle$ here. This quantum state can be prepared by the initialization algorithm in Ref [40] with $\mathcal{O}(L_i \log_2 L_i)$ standard gate operations or $\mathcal{O}(\log_2 L_i)$ steps with quantum random access memory method [41]. Then a series of multi-qubit controlled operators $\sum_{i=1}^{L_i} |i\rangle \langle i| P_i$ are applied onto the whole system, creating entanglement between the ancillary and working systems. The state of the whole system is transformed into $\left[|1\rangle (\alpha_1^{(i)} - \lambda_0) P_1 + \sum_{j=2}^{L_i} |j\rangle \alpha_j^{(i)} P_j \right] |\psi_0\rangle / \mathcal{C}$. Followed by the decoding operation realized with the Hardmard gates $H^{\otimes \log_2 L_i}$ on the ancillary system, we concern the output state of working system in the $\left|0^{\otimes \log_2 L_i}\right\rangle$ subspace of the ancillary system as

$$\frac{(\alpha_1^{(i)} - \lambda_0) P_1 + \sum_{j=2}^{L_i} \alpha_j^{(i)} P_j}{\mathcal{C}\sqrt{2^{L_i}}} |\psi_0\rangle = \frac{U_i |\psi_0\rangle}{\mathcal{C}\sqrt{2^{L_i}}} \tag{6}$$

and this means that we can realize the simulation of target operator by measuring the ancillary system in state $\left|0^{\otimes \log_2 L_i}\right\rangle$ with success probability $P_s^{(i)} = ||U_i |\psi_0\rangle||^2 / (\mathcal{C}^2 2^{L_i})$ at each iteration, where $||x||$ represents the modulus of vector x. We can also further increase the probability for obtaining target quantum states by quantum amplitude amplification technology [42, 43].

Then the output of this basic process will be the input for the next iteration, which needs to be repeated k_i times when determining the i-th eigenstate, and the final output state $\left|\widetilde{E}_i\right\rangle$ of the working system would be a good approximation to the eigenstate $|E_i\rangle$. Based on the output state, we can obtain its measurement values for each Pauli words $\epsilon_j^{(i)} = \left\langle \widetilde{E}_i \right| P_j \left| \widetilde{E}_i \right\rangle$ as the basic energy components, which are then used for calculating the approximate eigenvalues $\widetilde{E}_i$ and updating the state preparation operator for determining the next eigenstate. It is worth emphasizing that when we want to determine different energy-levels, only the operator V_i needs to be changed, which reduces the complexity and

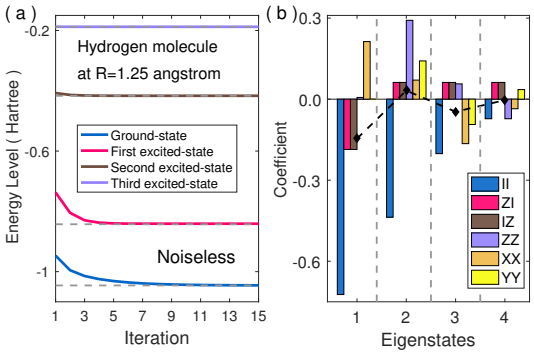

Figure 3: A simulation of the iteration process for hydrogen molecule without noise at the $R = 1.25$ angstrom. (a) The iteration processes for different energy-levels. (b) The updating parameter $\alpha_j^{(i)}$ under Pauli basis and the black diamond points represent the mean coefficients for different energy-levels.

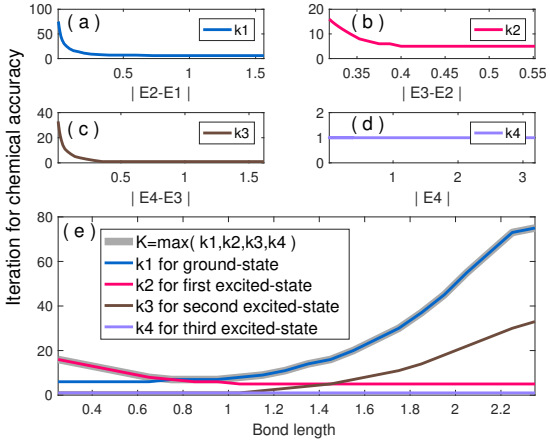

Figure 4: (a-d) The minimum iteration times k_i for realizing chemical accuracy when determining eigenenergy and its relation with the energy difference. (e) The maximum iteration times $K = \max\{k_i\}$ under different bond lengths (unit in angstrom).

resource cost during the iteration updating process. In addition to the programmable or updatable state preparation process, the other parts of our algorithm can be modularized in principle for determining the energy spectrum of different molecules. Moreover, the procedures for determining the i-th eigenstate in our FQESS algorithm is similar to that in FQE algorithm, and by updating the state preparation process using the energy output of last iteration, we extend the solution of the ground-state to the entire energy spectrum.

2.3 Complexity Analysis

The algorithm complexity for our FQESS algorithm includes qubit resources and gate complexity. For qubit resources, the number of ancillary qubits needed is $\log_2 L \leq 2n$, where $L = \max\{L_i\}$ is the maximum number of Pauli words in the Hamiltonian. Therefore, the total number of qubits in our algorithm is $\mathcal{O}(n + \log_2 L)$, no more than $3n$-qubits. As for the gate complexity in each basic process, we need $\mathcal{O}(L \log_2 L)$ single- and two-qubit gates for the encoding process [40] and $\mathcal{O}(nL \log_2 L)$ basic gates for entangling process [44, 45]. Consider another $\log_2 L$ Hardmard gates for decoding, the total basic gates required for the realization of U_i operator when obtaining the i-th energy-level is $\mathcal{O}(nL \log_2 L)$ for the FQESS algorithm. For the chemistry Hamiltonian of electrons with $L = \mathcal{O}(n^4)$, the gate complexity is $\mathcal{O}(n^5 \log_2 n)$. Moreover, to estimate the approximate eigenvalue $\widetilde{E}_i = \sum_{j=1}^{L_i} \alpha_j^{(i)} \epsilon_j^{(i)}$, we need $\mathcal{O}(L_i / P_s^{(i)} / \delta^2)$ measurements, where $P_s^{(i)}$ indicates the probability that all qubits of the auxiliary system are measured to be $|0\rangle$ quantum states, and $\delta \propto N^{-1/2}$ represents the statistical error of $\epsilon_j^{(i)}$ when N measurements are made [46].

3 Numerical Simulation

In this part, we present a demonstration of the FQESS algorithm for excited-states with the hydrogen and LiH molecules in the minimal STO-3G basis for a range of inter-nuclear separations to verify the feasibility and robustness of the algorithm. The fermionic Hamiltonian of hydrogen can be translated into qubit representation by Bravyi-Kitaev transformation [33], obtaining a two-qubit Hamiltonian as

$$\begin{aligned} H(R) =& \alpha_0^R + \alpha_1^R \sigma_z^{(1)} + \alpha_2^R \sigma_z^{(2)} + \alpha_3^R \sigma_z^{(1)} \otimes \sigma_z^{(2)} \\ &+ \alpha_4^R \sigma_x^{(1)} \otimes \sigma_x^{(2)} + \alpha_5^R \sigma_y^{(1)} \otimes \sigma_y^{(2)} \end{aligned} \tag{7}$$

where $\sigma_\beta^{(i)}$ $(\beta = x, y, z)$ is the Pauli operator acting on the i-th qubit and the real-valued coefficients α_i^R are functions of the inter-nuclear distance R [26]. Also, a six-qubit Hamiltonian for LiH molecule containing 118 Pauli words is obtained via the Jordan-Wigner transformation [32]. Moreover, numerical simulation results of larger molecules for H2O (12 qubits) and NH3 (14 qubits) in STO-6G basis set are presented in Appendix B. First, we apply our FQESS algorithm

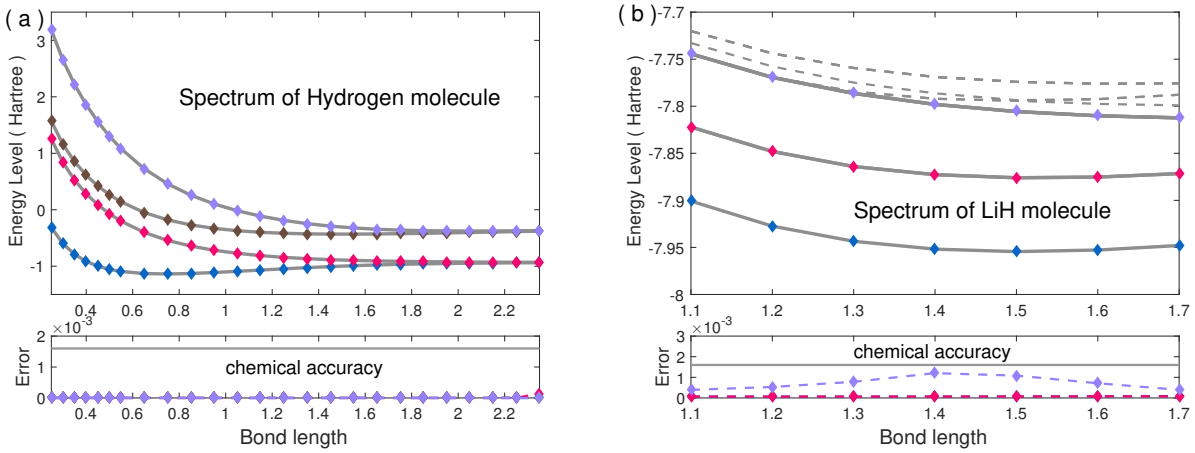

Figure 5: A simulation of hydrogen (a) and LiH (b) molecule spectrum without noise for a range of inter-nuclear separations (unit in angstrom). The exact values are obtained by Hamiltonian diagonalization and plotted in gray lines. The numerical results are plotted with circles. Errors between the numerical outputs and the theoretical expectations are shown in the bottom panel.

to the hydrogen molecule and plot the power iteration process for each eigenstate at $R = 1.25$ angstrom in the Figure 3, together with a updating parameter $\alpha_j^{(i)}$ under different Pauli basis. The initial state is chosen as $|\psi_0\rangle = |0\rangle \otimes |+\rangle$, where $|+\rangle$ is a eigenvector of σ_x matrix. It can be concluded that iteration processes can quickly converge to the target values. More importantly, the iteration times needed is less when the energy-level is high enough, especially for the last eigenstate, there is no need for extra iterations. This is due to that our algorithm eliminates the other eigen-components during the iteration process and the left new-constructed Hamiltonian has less eigen-components and is purer, which makes it easier to extract the remaining eigenstates. We need to analyze the properties related to the number of iterations. The Figure 4 shows the relationship between the number of iterations k_i required to achieve chemical accuracy (0.0016 Hartree) and the energy-level difference. It can be found that a larger energy-level interval generally requires fewer iterations, but the highest energy state requires only one iteration ($k_4 = 1$), independent of the energy-level difference. We also plot the iterations times with bond length and find the maximum times $K = \max\{k_i\}$. We will show below that our FQESS algorithm can achieve faster convergence compared with other typical hybrid variational quantum algorithms for excited-states.

We plot the whole spectrum of the hydrogen and LiH molecules for a wide range of inter-nuclear separations in Figure 5. We set $k_i = 600$ for better optimization results beyond chemical accuracy and the initial state for hydrogen is still $|\psi_0\rangle$ but for LiH molecule is $|+\rangle^{\otimes 6}$. By introducing suitable bias terms, we can find the energy-levels in turns, and the maximum differences for two molecules between the numerical outputs and the theoretical expectations are 0.000145 and 0.001203 Hartree, separately. Moreover, we study the effect of random noise term in the form $\sum_i^n \delta\alpha_i^R \sigma_z^{(i)}$, which is used to simulate decoherence noise with certain intensity [19, 31]. In each optimization, we set iteration times as $k_i = 600$ and these processes are repeated five times for average values, which is used as the output and the maximum deviation from the mean values are seen as error bars, as plotted in the Figure 6. We can conclude based on the output results that our algorithm is robust to the random noise and the fast convergence still can be achieved. The mean error of different eigenenergies between optimization results and theoretical expectations are 0.000978 and 0.000231 Hartree and the accuracy of most data points exceed the chemical accuracy.

Furthermore, we compare the FQESS algorithm with another two typical hybrid variational algorithms for excited-states, i.e. VQD and SSVQE algorithm. The ansatz circuit for these two algorithms is the hardware-efficient ansatz [13] and the classical optimization algorithm used

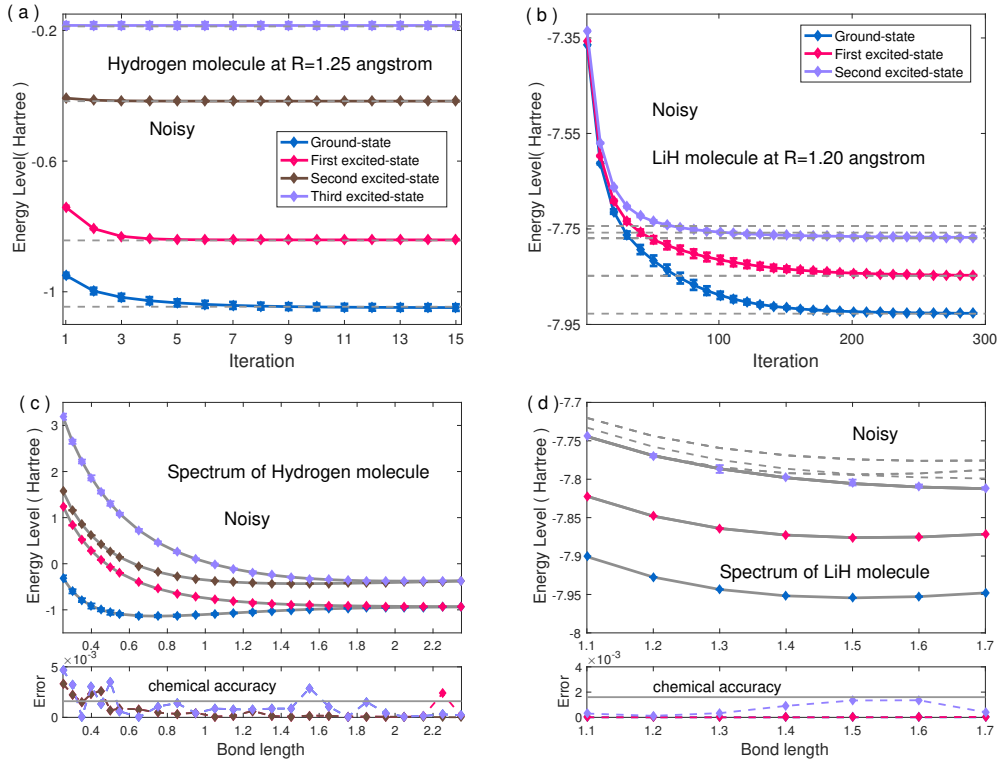

Figure 6: A simulation of the hydrogen and LiH molecule with noise. (a,b) The iteration processes for different energy-levels at a specific bond length. (c,d) The whole spectrum for a range of inter-nuclear separations (unit in angstrom). The exact values are obtained by Hamiltonian diagonalization and plotted by lines. The numerical results are plotted with circles and the maximum deviation from the mean values are used as error bars. Errors between the numerical outputs and the theoretical expectations are shown in the bottom panel.

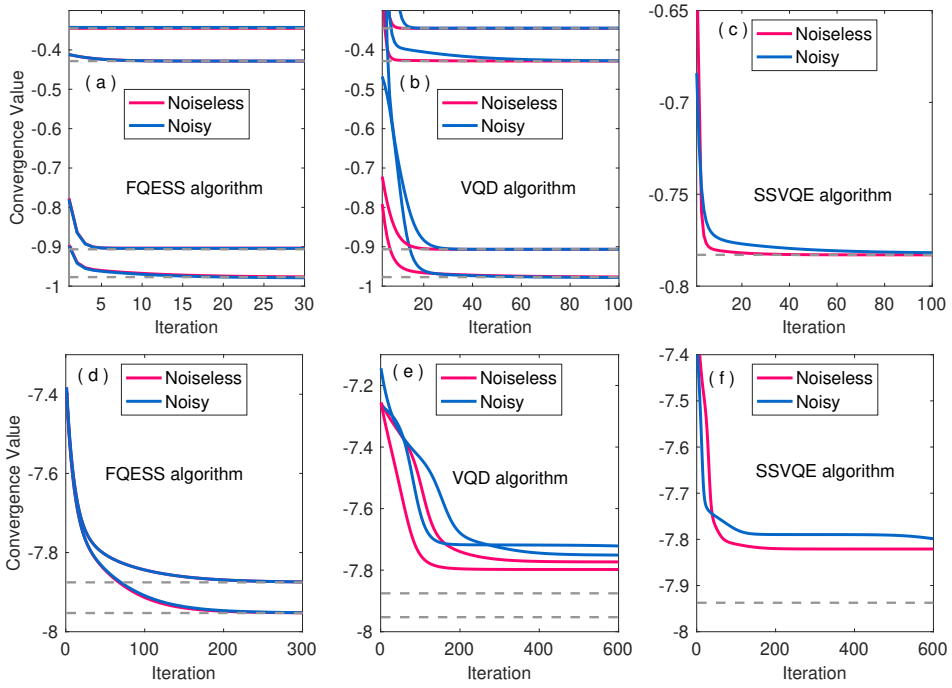

Figure 7: Comparison of algorithms for excited-states between the FQESS, VQD and SSVQE algorithms with hydrogen (a-c) and LiH molecule (d-f). The performances of these algorithms under noiseless and 10% noise are presented in red and blue lines, separately. The target convergence values labelled by gray dashed lines for FQESS and VQD algorithms are the eigenenergies of hydrogen molecule at $R = 1.65$ angstrom and LiH molecule at $R = 1.60$ angstrom, while target convergence value for SSVQE algorithm is a weighted average of energy eigenvalues.

is Newton gradient descent algorithm. For hydrogen molecule, the initial state for VQD algorithm is same to that of FQESS algorithm when determining various eigenstates. The four initial orthogonal states in the SSVQE algorithm are chosen as the eigenstates of P_1 and the corresponding weights for them are $w_1 = 0.4$, $w_2 = 0.3$, $w_3 = 0.2$, $w_4 = 0.1$. So the target convergence value for SSVQE algorithm is $\sum_{i=1}^{4} w_i E_i$. For LiH molecule, the convergence values for FQESS and VQD algorithms are the eigenenergies of LiH molecule at $R = 1.60$ angstrom, while target value for SSVQE algorithm is a weighted average ($w_1 = 0.8$, $w_2 = 0.2$) of the lowest two eigenvalues. The initial state for VQD and FQESS algorithm when determining various eigenstates is $|+\rangle^{\otimes 6}$ and the two initial orthogonal states for SSVQE algorithm are $|+-\rangle^{\otimes 3}$ and $|-+\rangle^{\otimes 3}$. The performances of these algorithms under noiseless and 10% noise for hydrogen and LiH molecules are presented in the Figure 7. We can find that our FQESS algorithm shows stronger robustness against noise and the iteration times needed is less, which means it can achieve a faster convergence compared with the other two algorithms for excited-states. Although the two hybrid variational algorithms can be improved by changing the ansatz circuit or classical optimization process, these enhancements require pre-selection based on some prior knowledge, which is a potential challenge in practical applications, while the construction of FQESS algorithm only depends on the form of the target chemical Hamiltonian. The non-variational nature can also ensure that the FQESS algorithm converges to the target states along the direction of the fastest gradient descent, avoiding barren plateau. In addition, our algorithm can avoid the key challenges of overlap estimation realized by swap test in the VQD algorithm, and the limited number of solvable excited-states caused by the difficulty of simultaneous optimization of ansatz in the SSVQE algorithm.

4 Experimental Demonstration

Here we demonstrate our FQESS algorithm with the real superconducting quantum computation chip on the Quafu quantum cloud platform [47]. Detail information about Quafu cloud platform can be found in the Appendix C.

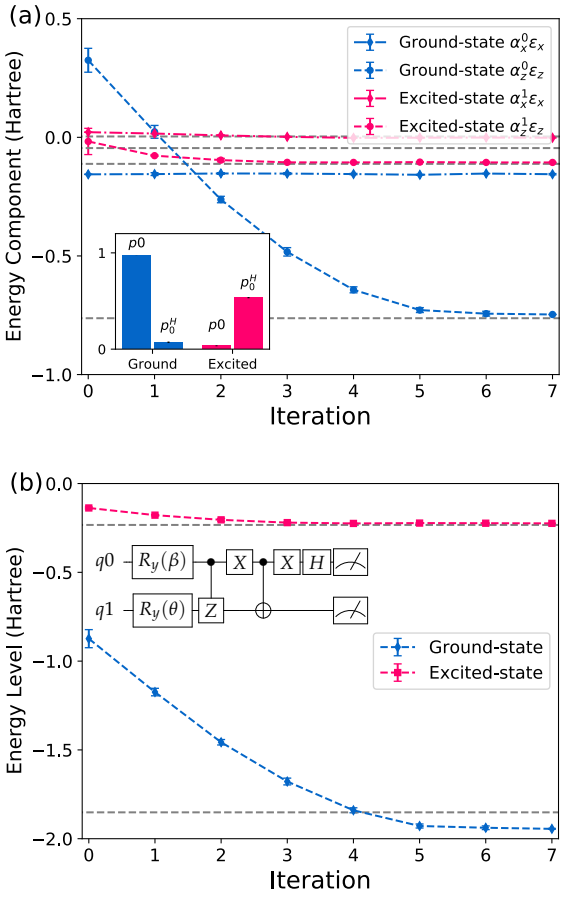

Figure 8: (a) Energy components during iteration and final probability distribution for the ground- and excited-state. (b) Experimental quantum circuit and iteration results of FQESS algorithm with hydrogen molecular on the superconducting quantum computation chips.

As a proof-of-principle experimental demonstration, we consider the singlet and spatial symmetry of ground state in the hydrogen molecular, and then only two configurations are relevant in the calculation, i.e. the ground-state configuration and the double excitation configuration. Then the simplified Hamiltonian can be expressed as a two-dimensional matrix $H = \alpha_0 + \alpha_x\sigma_x + \alpha_z\sigma_z$ in the Pauli basis with coefficients $\alpha_0 = -1.04235$, $\alpha_x = 0.1813$ and $\alpha_z = -0.78865$ [48]. Then a series of basic quantum logic gates can be applied as the quantum circuit introduced above and the encode operator on the ancillary qubit $[q0]$ is $R_y(\beta) = [\cos(\beta/2), -\sin(\beta/2); \sin(\beta/2), \cos(\beta/2)]$ with $\beta = -2.6897$ for the ground state. The iteration process can be realized by introducing a rotation operator $R_y(\theta)$ on the work qubit $[q1]$, which start from $|+\rangle$ state with $\theta = \pi/2$ initially.

The quantum processor will be called ten thousand times to obtain high-precision values in each setup and the experiment will be repeated three times to obtain error bars. As for the measurement, assume that the output quantum state of work system is $|\phi_{\rm I}\rangle$ and the experimentally-measurable distribution of $p0 = |\langle 0|\phi_{\rm I}\rangle|^2$ and $p1 = |\langle 1|\phi_{\rm I}\rangle|^2$ can be determined in the subspace of ancillary qubit. Then two energy components can be determined as $\epsilon_0 = \langle\phi_{\rm I}|\phi_{\rm I}\rangle = 1$, and $\epsilon_z = \langle\phi_{\rm I}|\,\sigma_z\,|\phi_{\rm I}\rangle = p0 - p1$. Because that $\epsilon_x = \langle\phi_{\rm I}|\,\sigma_x\,|\phi_{\rm I}\rangle = \langle\phi_{\rm I}|\,\mathcal{H}\sigma_z\mathcal{H}\,|\phi_{\rm I}\rangle$ where $\mathcal{H}$ represents Hardmard gate, we can repeat the same circuit but add $\mathcal{H}$ on work qubit to obtain $|\phi_{\mathcal{H}}\rangle = \mathcal{H}\,|\phi_{\rm I}\rangle$ with new probability distribution $p_0^{\mathcal{H}}$ and $p_1^{\mathcal{H}}$, and then $\epsilon_x = \langle\phi_{\mathcal{H}}|\,\epsilon_z\,|\phi_{\mathcal{H}}\rangle = p_0^{\mathcal{H}} - p_1^{\mathcal{H}}$. Therefore, the energy can be reconstructed as $E_{\rm exp} = \sum_{i=0,x,z}\alpha_i\epsilon_i$ experimentally. To realize the multi-step iteration, we need to repeat another same evolution process, but start with the output state in the last iteration. This can be realized by modifying the angle θ with formula $\theta = -2\arcsin(p1^{0.5})$. The experimental quantum circuit and iteration results of energy are plotted in the Figure 8, which show a good agreement with the theoretical expectations.

5 Discussion

In summary, we have proposed a full quantum algorithm in circuit frame for the excited-states of quantum chemistry, termed FQESS algorithm. Compared with the hybrid variational algorithm, our method does not need the classical optimizer and all the calculations are performed on the quantum computer. The non-variational characteristic makes the algorithm converge to the target states along the direction of the fastest gradient descent, avoiding the barren plateau phenomenon. The output results of energy for the last energy-level can be used as the updating parameter for determining the next energy-level, and the only difference between different iterations for various eigenstates is the state preparation process of ancillary system, which can be simply realized by modifying the encoding operator. We present a numerical simulation with the hydrogen, LiH, H2O and NH3 molecules to demonstrate the feasibility and robustness of the algorithm. A proof-of-principle experiment has also been demonstrated on the practical superconducting quantum chip, and the results show a good agreement with theoretical expectations. Our algorithm fills the last step of solving quantum chemistry problems based on different algorithm frames and can be used as a generalized Hamiltonian diagonalization scheme on the future fault-tolerant quantum computers.

Acknowledgements

S. W. and G. L. are corresponding authors. We acknowledge the support from the National Natural Science Foundation of China under Grants No. 12005015 and No. 11974205; the National Key R&D Plan (2021YFB2801800); the National Key Research and Development Program of China (2017YFA0303700); Beijing Advanced Innovation Center for Future Chip (ICFC). We gratefully acknowledge support from the Extreme Condition User Facility in Beijing and Quafu cloud platform for quantum computation. S. W. acknowledges the Beijing Nova Program under Grants No. 20230484345. H. F. acknowledge the support from the National Natural Science Foundation of China under Grants No. T2121001 and No. 92265207. Z. W. acknowledge the support from China Postdoctoral Science Foundation No. 2022TQ0036, National Natural Science Foundation of China No. 12247168 and No. 92265207.

A Theory of the FQESS Algorithm

The eigen-equation for an $n \times n$ matrix A can be written as $Au^{(i)} = \lambda_i u^{(i)}$, where λ_i is eigenvalue and $u^{(i)}$ is the corresponding eigenvector. For an arbitrarily selected vector $x^{(0)}$, it can always be decomposed in the eigenvector basis as $x^{(0)} = \sum_i^n a_i u^{(i)}$. Then we can multiply the matrix A with k times to $x^{(0)}$ and we have

$$x^{(k)} = A^k x^{(0)} = \lambda_1^k\Big[a_1 u^{(1)} + \sum_{i=2}^{n} a_i (\frac{\lambda_i}{\lambda_1})^k u^{(i)}\Big] \quad (8)$$

Suppose that the absolute values of the eigenvalues satisfy the relation $|\lambda_1| > |\lambda_2| \geq \cdots \geq |\lambda_n|$, then $\lim_{k\to\infty}(\lambda_i/\lambda_1)^k = 0$. Therefore, the second item in equation (8) will vanish when we apply enough times of matrix A. Under the assumption that the initial vector has finite overlap with the targeted eigenvector ($a_1 \neq 0$), the remaining term will be proportional to the eigenvector $u^{(1)}$ with the biggest eigenvalue, except for

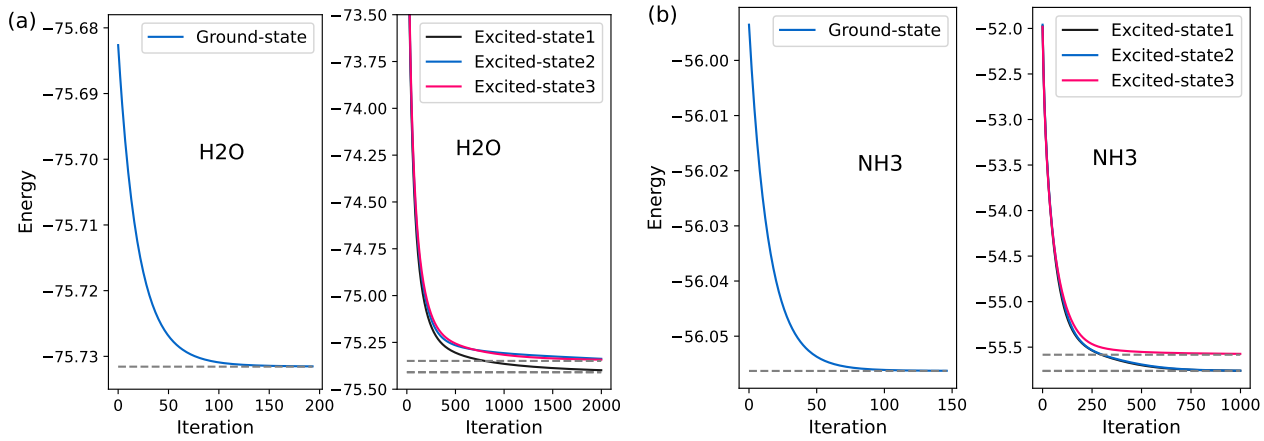

Figure 9: Numerical simulations of the 12-qubit H2O (a) and 14-qubit NH3 (b) molecules. The left side in each panel shows the iteration processes of energy (unit in Hartree) for ground-states, while the right side shows that for excited-states. The target convergence energies obtained by Hamiltonian diagonalization are indicated by gray dashed lines.

a coefficient, which can be eliminated by normalization. The process presented above is termed power iteration method, which is a common iterative method to calculate the maximum absolute value of eigenvalue and the corresponding eigenvector (principal component) of the matrix [49]. This intuitive and elegant method works well for the eigenvector estimation of the large and sparse matrices. We take this method as the basic eigencomponent extracter of the chemical Hamiltonian in the FQESS algorithm.

In addition, the method involved in the FQESS algorithm can also be interpreted from the perspective of quantum gradient descent [19]. The target function can be expressed as a quadratic optimization problem as $f(|X\rangle) = \langle X| H |X\rangle$, and then the state evolving along the direction of the gradient of target function can be expressed as

$$\left|X^{t+1}\right\rangle = \left|X^{t}\right\rangle - \gamma \nabla f(\left|X^{t}\right\rangle) = (I - 2\gamma H)\left|X^{t}\right\rangle \tag{9}$$

where γ represents the learning rate. If the bias parameter is set as $\lambda_0 = 1/2\gamma$ and ignore an unimportant multiplying factor, the gradient operator $U_g = (I - 2\gamma H)$ will be same to the operator U_i in equation (4), both of which are linear combinations of unitary operators. Therefore, the iteration process of FQESS algorithm can also be regarded as the process of quantum state converging to the specific eigenstate along the gradient direction of objective function.

B Simulation of H2O and NH3 molecules

To demonstrate the performance of the FQESS algorithm in larger systems, we offer the numerical simulations with 12-qubit H2O and 14-qubit NH3 molecules in STO-6G basis set here, providing additional support for the effectiveness of our algorithm. For the ground-states, we start from Hartree-Fock states, and use random initial quantum states in excited-states for better convergence. Other setup is same to the simulation in the hydrogen and LiH molecules. As shown in the Figure 9, the FQESS algorithm can well converge to the target solution of ground-states and excited-states, indicating that the algorithm is feasible to solve the energy spectrum in larger molecular systems. Compared with the exact solutions obtained by Hamiltonian diagonalization, the error of ground-state energy for H2O (NH3) molecule is 0.000043 (0.000029) Hartree, and the average error of excited-states is 0.001163 (0.000399) Hartree, both reaching the chemical accuracy.

C Quafu Quantum Cloud Platform

Quafu is an open cloud platform for quantum computation [47], which provides four specifications of superconducting quantum processors currently. Three of them support general quantum logical gates, which are 10-qubits and 18-qubits processors with one-dimensional chain structure

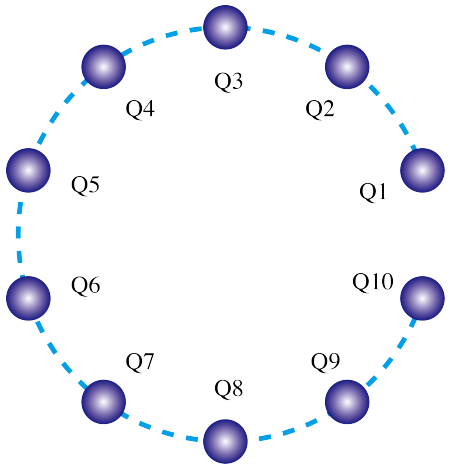

Figure 10: The topological structure of quantum processor P-10. Each qubit capacitively coupled to its nearest-neighbors.

named P-10 and P-18, and a 50+ qubits processor with a two-dimensional honeycomb structure named P-50. In this work, we use the first two qubits of P-10 quantum processor, whose topological structure is shown in the Figure 10. The processor consists of ten transmon qubits ($Q_1 - Q_{10}$) arrayed in a row, with each qubit capacitively coupled to its nearest-neighbors. Each transmon qubit can be modulated in frequency from about 4 to 5.7 GHz and excited to the excited state individually. All qubits can be probed though a common transmission line connected to their own readout resonators. The qubit parameters and coherence performance can be found in the Table 1. The idle frequencies of each qubit (ω_j^{10}) are designed to reduce residual coupling strength from other qubits.

References

[1] Paul Benioff. The computer as a physical system: A microscopic quantum mechanical hamiltonian model of computers as represented by turing machines. *Journal of statistical physics*, 22(5):563–591, 1980. DOI: 10.1007/BF01011339.

[2] Richard P Feynman. Simulating physics with computers. *Int J Theor Phys*, 21(1): 467–488, 1982. DOI: 10.1007/BF02650179.

[3] Peter W Shor. Polynomial-time algorithms for prime factorization and discrete logarithms on a quantum computer. *SIAM review*, 41(2):303–332, 1999. DOI: 10.1137/S0036144598347011.

[4] Lov K Grover. Quantum mechanics helps in searching for a needle in a haystack. *Physical review letters*, 79(2):325, 1997. DOI: 10.1103/PhysRevLett.79.325.

[5] Gui Lu Long, Yan Song Li, Wei Lin Zhang, and Li Niu. Phase matching in quantum searching. *Physics Letters A*, 262(1):27–34, 1999. DOI: 10.1016/S0375-9601(99)00631-3.

[6] Aram W Harrow, Avinatan Hassidim, and Seth Lloyd. Quantum algorithm for linear systems of equations. *Physical review letters*, 103(15):150502, 2009. DOI: 10.1103/PhysRevLett.103.150502.

[7] Yiğit Subaşı, Rolando D Somma, and Davide Orsucci. Quantum algorithms for systems of linear equations inspired by adiabatic quantum computing. *Physical review letters*, 122(6):060504, 2019. DOI: 10.1103/PhysRevLett.122.060504.

[8] Yudong Cao, Jonathan Romero, Jonathan P Olson, Matthias Degroote, Peter D Johnson, Mária Kieferová, Ian D Kivlichan, Tim Menke, Borja Peropadre, Nicolas PD Sawaya, et al. Quantum chemistry in the age of quantum computing. *Chemical reviews*, 119(19):10856–10915, 2019. DOI: 10.1021/acs.chemrev.8b00803.

[9] Sam McArdle, Suguru Endo, Alán Aspuru-Guzik, Simon C Benjamin, and Xiao Yuan. Quantum computational chemistry. *Reviews of Modern Physics*, 92(1):015003, 2020. DOI: 10.1103/RevModPhys.92.015003.

[10] Bela Bauer, Sergey Bravyi, Mario Motta, and Garnet Kin-Lic Chan. Quantum algorithms for quantum chemistry and quantum materials science. *Chemical Reviews*, 120(22):12685–12717, 2020. DOI: 10.1021/acs.chemrev.9b00829.

[11] Alberto Peruzzo, Jarrod McClean, Peter Shadbolt, Man-Hong Yung, Xiao-Qi Zhou, Peter J Love, Alán Aspuru-Guzik, and Jeremy L O'brien. A variational eigenvalue solver on a photonic quantum processor. *Nature communications*, 5(1):1–7, 2014. DOI: 10.1038/ncomms5213.

[12] Peter JJ O'Malley, Ryan Babbush, Ian D Kivlichan, Jonathan Romero, Jarrod R McClean, Rami Barends, Julian Kelly, Pedram Roushan, Andrew Tranter, Nan Ding, et al.

qubit	Q_1	Q_2	Q_3	Q_4	Q_5	Q_6	Q_7	Q_8	Q_9	Q_{10}
$\omega_j^s/2\pi$ (GHz)	5.536	5.069	5.660	4.742	5.528	4.929	5.451	4.920	5.540	4.960
$\omega_j^{10}/2\pi$ (GHz)	5.456	4.424	5.606	4.327	5.473	4.412	5.392	4.319	5.490	4.442
$\omega_j^r/2\pi$ (GHz)	5.088	4.702	5.606	4.466	5.300	4.804	5.177	4.697	5.474	4.819
$\eta_j/2\pi$ (GHz)	0.250	0.207	0.251	0.206	0.251	0.203	0.252	0.204	0.246	0.208
$g_{j,j+1}/2\pi$ (MHz)	12.07	11.58	10.92	10.84	11.56	10.00	11.74	11.70	11.69	-
$T_{1,j}$ (us)	20.0	52.5	15.9	16.3	36.9	44.4	30.8	77.7	22.8	25.0
$T_{2,j}^*$ (us)	8.60	1.48	9.11	2.10	12.8	2.73	15.7	1.88	4.49	2.05
$F_{0,j}$ (%)	98.90	98.32	98.67	95.30	97.00	95.47	97.00	96.37	98.33	97.13
$F_{1,j}$ (%)	92.90	92.30	92.97	91.53	86.17	87.93	93.40	93.37	94.63	92.07
$F_{j,j+1}$ (%)	94.2	97.8	96.6	97.3	96.8	97.0	94.5	93.2	96.0	-

Table 1: Device parameters. ω_j^s shows the maximum frequency of Q_j. ω_j^{10} corresponds to the idle frequency of Q_j. ω_j^r shows the resonant frequency of Q_j during readout. η_j corresponds to the anharmonicity of Q_j. $g_{j,j+1}$ is the coupling strength between nearest-neighbor qubits. $T_{1,j}$ and $T_{2,j}^*$ represent the relaxation time and coherence time of Q_j. $F_{0,j}$ and $F_{1,j}$ are readout fidelities of Q_j in $|0\rangle$ and $|1\rangle$. $F_{j,j+1}$ represents the fidelity of CZ gate composed of Q_i and Q_j, which is obtianed by randomized benchmarking.

Scalable quantum simulation of molecular energies. *Physical Review X*, 6(3):031007, 2016. DOI: 10.1103/PhysRevX.6.031007.

[13] Abhinav Kandala, Antonio Mezzacapo, Kristan Temme, Maika Takita, Markus Brink, Jerry M Chow, and Jay M Gambetta. Hardware-efficient variational quantum eigensolver for small molecules and quantum magnets. *Nature*, 549(7671):242–246, 2017. DOI: 10.1038/nature23879.

[14] Marco Cerezo, Andrew Arrasmith, Ryan Babbush, Simon C Benjamin, Suguru Endo, Keisuke Fujii, Jarrod R McClean, Kosuke Mitarai, Xiao Yuan, Lukasz Cincio, et al. Variational quantum algorithms. *Nature Reviews Physics*, pages 1–20, 2021. DOI: 10.1038/s42254-021-00348-9.

[15] Xavi Bonet-Monroig, Ramiro Sagastizabal, M Singh, and TE O'Brien. Low-cost error mitigation by symmetry verification. *Physical Review A*, 98(6):062339, 2018. DOI: 10.1103/PhysRevA.98.062339.

[16] Harper R Grimsley, Sophia E Economou, Edwin Barnes, and Nicholas J Mayhall. An adaptive variational algorithm for exact molecular simulations on a quantum computer. *Nature communications*, 10(1):1–9, 2019. DOI: 10.1038/s41467-019-10988-2.

[17] Ho Lun Tang, VO Shkolnikov, George S Barron, Harper R Grimsley, Nicholas J Mayhall, Edwin Barnes, and Sophia E Economou. qubit-adapt-vqe: An adaptive algorithm for constructing hardware-efficient ansätze on a quantum processor. *PRX Quantum*, 2 (2):020310, 2021. DOI: 10.1103/PRXQuantum.2.020310.

[18] Mateusz Ostaszewski, Edward Grant, and Marcello Benedetti. Structure optimization for parameterized quantum circuits. *Quantum*, 5:391, 2021. DOI: 10.22331/q-2021-01-28-391.

[19] Shijie Wei, Hang Li, and GuiLu Long. A full quantum eigensolver for quantum chemistry simulations. *Research*, 2020, 2020. DOI: 10.34133/2020/1486935.

[20] Patrick Rebentrost, Maria Schuld, Leonard Wossnig, Francesco Petruccione, and Seth Lloyd. Quantum gradient descent and newton's method for constrained polynomial optimization. *New Journal of Physics*, 21(7):073023, 2019. DOI: 10.1088/1367-2630/ab2a9e.

[21] Oscar Higgott, Daochen Wang, and Stephen Brierley. Variational quantum computation of excited states. *Quantum*, 3:156, 2019. DOI: 10.22331/q-2019-07-01-156.

[22] Tyson Jones, Suguru Endo, Sam McArdle, Xiao Yuan, and Simon C Benjamin. Variational quantum algorithms for discovering hamiltonian spectra. *Physical Review A*, 99(6):062304, 2019. DOI: 10.1103/PhysRevA.99.062304.

[23] Ken M Nakanishi, Kosuke Mitarai, and Keisuke Fujii. Subspace-search variational quantum eigensolver for excited states. *Physical Review Research*, 1(3):

033062, 2019. DOI: 10.1103/PhysRevResearch.1.033062.

[24] Robert M Parrish, Edward G Hohenstein, Peter L McMahon, and Todd J Martínez. Quantum computation of electronic transitions using a variational quantum eigensolver. *Physical review letters*, 122(23):230401, 2019. DOI: 10.1103/PhysRevLett.122.230401.

[25] Jarrod R McClean, Mollie E Kimchi-Schwartz, Jonathan Carter, and Wibe A De Jong. Hybrid quantum-classical hierarchy for mitigation of decoherence and determination of excited states. *Physical Review A*, 95(4):042308, 2017. DOI: 10.1103/PhysRevA.95.042308.

[26] James I Colless, Vinay V Ramasesh, Dar Dahlen, Machiel S Blok, Mollie E Kimchi-Schwartz, Jarrod R McClean, Jonathan Carter, Wibe A de Jong, and Irfan Siddiqi. Computation of molecular spectra on a quantum processor with an error-resilient algorithm. *Physical Review X*, 8(1):011021, 2018. DOI: 10.1103/PhysRevX.8.011021.

[27] Pejman Jouzdani, Stefan Bringuier, and Mark Kostuk. A method of determining excited-states for quantum computation. *arXiv preprint arXiv:1908.05238*, 2019. DOI: 10.48550/arXiv.1908.05238.

[28] Pauline J Ollitrault, Abhinav Kandala, Chun-Fu Chen, Panagiotis Kl Barkoutsos, Antonio Mezzacapo, Marco Pistoia, Sarah Sheldon, Stefan Woerner, Jay M Gambetta, and Ivano Tavernelli. Quantum equation of motion for computing molecular excitation energies on a noisy quantum processor. *Physical Review Research*, 2(4):043140, 2020. DOI: 10.1103/PhysRevResearch.2.043140.

[29] Dan-Bo Zhang, Bin-Lin Chen, Zhan-Hao Yuan, and Tao Yin. Variational quantum eigensolvers by variance minimization. *Chinese Physics B*, 31(12):120301, 2022. DOI: 10.1088/1674-1056/ac8a8d.

[30] Saad Yalouz, Emiel Koridon, Bruno Senjean, Benjamin Lasorne, Francesco Buda, and Lucas Visscher. Analytical nonadiabatic couplings and gradients within the state-averaged orbital-optimized variational quantum eigensolver. *Journal of chemical theory and computation*, 18(2):776–794, 2022. DOI: 10.1021/acs.jctc.1c00995.

[31] Jingwei Wen, Dingshun Lv, Man-Hong Yung, and Gui-Lu Long. Variational quantum packaged deflation for arbitrary excited states. *Quantum Engineering*, page e80, 2021. DOI: 10.1002/que2.80.

[32] Pascual Jordan and Eugene Paul Wigner. über das paulische äquivalenzverbot. In *The Collected Works of Eugene Paul Wigner*, pages 109–129. Springer, 1993. DOI: 10.1007/978-3-662-02781-3_9.

[33] Sergey B Bravyi and Alexei Yu Kitaev. Fermionic quantum computation. *Annals of Physics*, 298(1):210–226, 2002. DOI: 10.1006/aphy.2002.6254.

[34] Long Gui-Lu. General quantum interference principle and duality computer. *Communications in Theoretical Physics*, 45(5):825, 2006. DOI: 10.1088/0253-6102/45/5/013.

[35] Long Gui-Lu and Liu Yang. Duality computing in quantum computers. *Communications in Theoretical Physics*, 50(6):1303, 2008. DOI: 10.1088/0253-6102/50/6/11.

[36] Long Gui-Lu, Liu Yang, and Wang Chuan. Allowable generalized quantum gates. *Communications in Theoretical Physics*, 51(1):65, 2009. DOI: 10.1088/0253-6102/51/1/13.

[37] Andrew M Childs and Nathan Wiebe. Hamiltonian simulation using linear combinations of unitary operations. *arXiv preprint arXiv:1202.5822*, 2012. DOI: 10.48550/arXiv.1202.5822.

[38] Jingwei Wen, Chao Zheng, Xiangyu Kong, Shijie Wei, Tao Xin, and Guilu Long. Experimental demonstration of a digital quantum simulation of a general $\mathcal{PT}$-symmetric system. *Physical Review A*, 99(6):062122, 2019. DOI: 10.1103/PhysRevA.99.062122.

[39] Jingwei Wen, Guoqing Qin, Chao Zheng, Shijie Wei, Xiangyu Kong, Tao Xin, and Guilu Long. Observation of information flow in the anti-$\mathcal{PT}$-symmetric system with nuclear spins. *npj Quantum Information*, 6(1):1–7, 2020. DOI: 10.1038/s41534-020-0258-4.

[40] Gui-Lu Long and Yang Sun. Efficient scheme for initializing a quantum register with an arbitrary superposed state. *Physical Review A*, 64(1):014303, 2001. DOI: 10.1103/PhysRevA.64.014303.

[41] Vittorio Giovannetti, Seth Lloyd, and

Lorenzo Maccone. Quantum random access memory. *Physical review letters*, 100 (16):160501, 2008. DOI: 10.1103/PhysRevLett.100.160501.

[42] Gilles Brassard, Peter Hoyer, Michele Mosca, and Alain Tapp. Quantum amplitude amplification and estimation. *Contemporary Mathematics*, 305:53–74, 2002. DOI: 10.1090/conm/305/05215.

[43] Dominic W Berry, Andrew M Childs, Richard Cleve, Robin Kothari, and Rolando D Somma. Simulating hamiltonian dynamics with a truncated taylor series. *Physical review letters*, 114(9):090502, 2015. DOI: 10.1103/PhysRevLett.114.090502.

[44] Tao Xin, Shi-Jie Wei, Julen S Pedernales, Enrique Solano, and Gui-Lu Long. Quantum simulation of quantum channels in nuclear magnetic resonance. *Physical Review A*, 96(6):062303, 2017. DOI: 10.1103/PhysRevA.96.062303.

[45] Shi-Jie Wei, Tao Xin, and Gui-Lu Long. Efficient universal quantum channel simulation in ibm's cloud quantum computer. *Science China Physics, Mechanics & Astronomy*, 61 (7):1–10, 2018. DOI: 10.1007/s11433-017-9181-9.

[46] Mario Napolitano, Marco Koschorreck, Brice Dubost, Naeimeh Behbood, RJ Sewell, and Morgan W Mitchell. Interaction-based quantum metrology showing scaling beyond the heisenberg limit. *Nature*, 471(7339):486–489, 2011. DOI: 10.1038/nature09778.

[47] Detail information about Quafu cloud platform can be found at website, github, and document.

[48] Jiangfeng Du, Nanyang Xu, Xinhua Peng, Pengfei Wang, Sanfeng Wu, and Dawei Lu. Nmr implementation of a molecular hydrogen quantum simulation with adiabatic state preparation. *Physical review letters*, 104(3):030502, 2010. DOI: 10.1103/PhysRevLett.104.030502.

[49] Maysum Panju. Iterative methods for computing eigenvalues and eigenvectors. *arXiv preprint arXiv:1105.1185*, 2011. DOI: 10.48550/arXiv.1105.1185.